photonics

Communication

Ultra-Broadband NPE-Based Femtosecond Fiber Laser

Sergei I. Abdrakhmanov [1,2], Vladislav D. Efremov [1,2], Alexey G. Kuznetsov [1], Denis S. Kharenko [1,2,*] and Sergey A. Babin [1,2]

[1] Institute of Automation and Electrometry SB RAS, 1 Acad. Koptyug Ave., 630090 Novosibirsk, Russia
[2] Department of Physics, Novosibirsk State University, 1 Pirogova St., 630090 Novosibirsk, Russia
* Correspondence: kharenko@iae.nsk.su

Abstract: A dissipative soliton mode-locked Yb-doped fiber laser is investigated experimentally and numerically from the point of view of generating ultra-broadband ultrashort pulses. An energy up to 2.2 nJ and a spectral bandwidth over 60 nm (at the −10 dB level) were obtained experimentally without dispersion compensation in the cavity. Almost a 100-fold compression coefficient has been achieved, so the resulting pulse duration was 149 fs. The numerical simulation has shown that a further scaling up to 3.5 nJ and a 100 nm spectral bandwidth is possible by reducing the low power transmission coefficient of the NPE-based SAM and increasing the amplification. At the same time, the tolerance of the SAM to a low power radiation is responsible for the transition to a multi-pulse operation regime.

Keywords: fiber lasers; mode-locked lasers; ultrashort pulses

check for updates

Citation: Abdrakhmanov, S.I.; Efremov, V.D.; Kuznetsov, A.G.; Kharenko, D.S.; Babin, S.A. Ultra-Broadband NPE-Based Femtosecond Fiber Laser. *Photonics* **2023**, *10*, 85. https://doi.org/10.3390/photonics10010085

Received: 5 December 2022
Revised: 6 January 2023
Accepted: 10 January 2023
Published: 12 January 2023

1. Introduction

Over the last two decades, fiber lasers have been intensively studied as a relatively simple and reliable source of powerful femtosecond pulses. Such lasers are already widely used in various fields such as micromachining, nonlinear microscopy, optical imaging, etc., [1–3] due to controllable phase-matching conditions and nonlinearity, the advanced all-fiber design of extremely fast saturable absorbers, a high beam quality, and a compact design. There are various configurations and approaches for a wide range of characteristics, but all-normal dispersion Yb-doped fiber lasers are among the most successful in terms of their high peak and average powers [4–8]. However, solid state ultrashort lasers are still a workhorse when a high quality temporal profile for a duration less than 50 fs and a high energy of more than 1 mJ is required.

A typical pulse energy of a fiber master oscillator is several nJ [9]. It can be scaled effectively by cavity lengthening and increasing the fiber mode-field diameter [4,10–12]. In addition, these schemes frequently use a spectral filter to increase the stability of mode locking. In depends on the ratio of a filter bandwidth and an output spectra bandwidth [13]; the pulses generated in these cavities can be classified as highly chirped dissipative solitons [14] or similaritons [15,16]. As for the spectral width, its typical value is about 20 nm, which gives the practical pulse duration of about 200 fs. Even shorter (less than 40 fs) pulses in Yb-doped fiber lasers can be obtained by using intracavity dispersion compensation [17], self-similar evolution together with adaptive compression [18], and special techniques such as the direct control of mode-locking states by a spatial light modulator [19]. It is interesting to note that the mode-locking state in all these lasers was driven by the nonlinear polarization evolution (NPE) effect, yet there are no papers exploring the extremely short pulse duration obtained by other saturable absorption mechanisms. The exception is the Mamyshev oscillator [20], which demonstrates outstanding parameters both in terms of its pulse duration and energy [7,8,21]. Additional spectral broadening up to 400 nm (at −20 dB) can be achieved by using highly nonlinear photonic-crystal fiber. As a result, the output pulses were compressed down to a few cycle durations of 17 fs [22]. The authors concluded that such a superior performance has been achieved, among other things, due to the "perfect" saturable absorber action of the Mamyshev oscillator. However, what this actually means in terms of the transmission function remains unknown and why such significant results have not yet been demonstrated using another kind of saturable absorber.

Here we report on the experimental and numerical investigation of the dissipative soliton regime in an NPE mode-locked Yb-doped fiber laser with a pulse energy of 2.2 nJ, a duration of 14 ps, and a spectral bandwidth over 60 nm (at the −10 dB level) achieved in a relatively long cavity (almost 15 m) without dispersion compensation. After dechirping by the grating compressor, the pulse width reduced to ∼140 fs with the potential for a further compression by third-order dispersion compensation. Our numerical modeling demonstrates a quantitative agreement with the experimental data and predicts for the first time the possibility of a 100 nm pulse generation and increasing the contrast of the self-amplitude modulator transmission function, which is contrary to the previously reported route, to minimize the pulse duration by reducing the GVD [23]. Such a regime could be used to improve the performance of femtosecond fiber lasers in terms of their pulse duration; it would also be useful if we could find a method for their application in fields where a broadband laser is required, such as multiphoton and time-resolved microscopy, harmonic generation, and material nano-processing.

2. Experimental Scheme and Results

The scheme of the oscillator is shown in Figure 1a. The laser is pumped by a multimode laser diode with a power up to 8 W at 980 nm through the pump combiner with a standard polarization maintaining (PM) signal fiber. The 81 cm long piece of active double-clad Yb-doped PM fiber also has standard 6/125 µm core/cladding diameters and absorption at 976 nm of 2.1 dB/m (IXF-2CF-Yb-PM-6-130, iXblue Inc., Six-Fours-les-Plages, France). NPE in a 76 cm long piece of SMF (Hi 1060, Nufern, East Granby, CT, USA) with a polarization controller (PC) and a polarizing beam splitter (PBS) which provides the mode-locking of the laser by the appropriate adjustment of the PC. The rest of the cavity consists of a passive PM fiber (PM 980) as in the previous work [11,12] to prevent NPE overdriving [24]. To improve the stability of the laser, we used a spectral filter based on diffraction grating (GR25-1210, Thorlabs, NJ, USA) and the dual fiber collimator (AFR Inc., Zhuhai, China). This kind of filter consists of two elements of bulk optics only and has already shown a great performance in terms of its contrast and tunability [25–27]. The central wavelength was selected to be 1043 nm. The bandwidth at the −3 dB level was equal to 1.62 nm (see Figure 1b) and was determined by a period of selected grating. The 1% coupler output port (connected to the 50% coupler) and the PBS output (the NPE rejection port) were utilized to control the stability of the mode-locking by observing a radio frequency (RF) spectrum and a pulse train correspondingly. The 99% coupler output port served as the main laser output and was used to measure the optical spectra, pulse duration, and output power. The PBS output and 99% coupler output were implemented using optical isolators to avoid back-reflections, which had a detrimental effect on the laser stability.

Optical spectrum measurements were performed by a Yokogawa AQ6370 optical spectrum analyzer. The RF spectrum was measured by a Keysight N9010A radio frequency analyzer in combination with the 5-GHz bandwidth photodiode (DET08CFC/M, Thorlabs, NJ, USA). The temporal pulse characteristics were obtained by the Mesaphotonics FROGscan instrument which applies the frequency-resolved optical gating (FROG) technique by the BBO crystal with a thickness of 200 µm. Pulse dechirping was implemented via an external double-pass compressor based on a diffraction grating pair (Spectrogon, PC 1500 NIR).

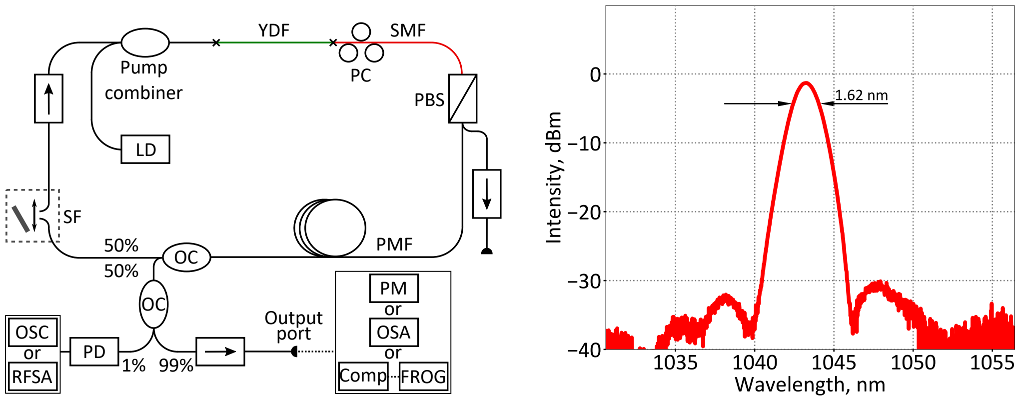

(**a**) (**b**)

Figure 1. Scheme of the experimental setup (**a**): LD—laser diode, YDF—double-clad Yb-doped fiber, PC—polarization controller, SMF—single-mode fiber, PBS—polarizing beam splitter, PMF—polarization-maintaining fiber, OC—optical coupler, SF—spectral filter, PD—photodiode, OSC—oscilloscope, RFSA—radio frequency spectrum analyzer, PM—power meter, OSA—optical spectrum analyzer, comp—pulse compressor, FROG—pulse duration measurement system; transmission spectrum of the spectral filter (**b**).

During the experiments, we achieved the generation of a stable single-pulse highly chirped soliton by the proper adjustment of the PC. Mode-locking occurs at a pump power above 4 W. The average output power and pulse repetition rate are about 27.3 mW and 13.5 MHz, respectively, which corresponds to a pulse energy of 2.2 nJ. The measured output spectrum is depicted in Figure 2a (solid red line); it has a width of 57 nm at the −10 dB level for 4.3 W pump power. Increasing the pump power to 4.5 W and slight adjustments of the PC led to a further spectrum broadening of up to 63 nm, which is more than twice as high as the value obtained previously in a similar scheme [28]. The corresponding output signal power is ∼31.4 mW. A further increase in the pump power leads to a multi-pulse operation regime. As far as we know, the spectrum of this DS is the widest among the other DS Yb-doped fiber systems and is one of the widest among Yb-doped passively mode-locked fiber lasers [19,29–31]. The RF spectrum of the laser is shown in Figure 2b. Its signal-to-noise ratio is as high as 75 dB, which confirms an excellent mode-locking stability.

The FROG trace was off due to the limited range of our measurement equipment, so it was not able to retrieve the phase and pulse shape, but the pulse duration was retrieved from the FROG traces simplified to the auto-correlation function by summing up the intensity of all the wavelengths at each time delay. For the chirped pulse, it is about 14 ps (Figure 2c). The dechirped pulse duration is about 149 fs (Figure 2d). So, the measured value of the chirp parameter is almost 100. The general form of the FROG trace (see inset in Figure 2d) indicates that a further pulse compression is limited by third-order dispersion [32].

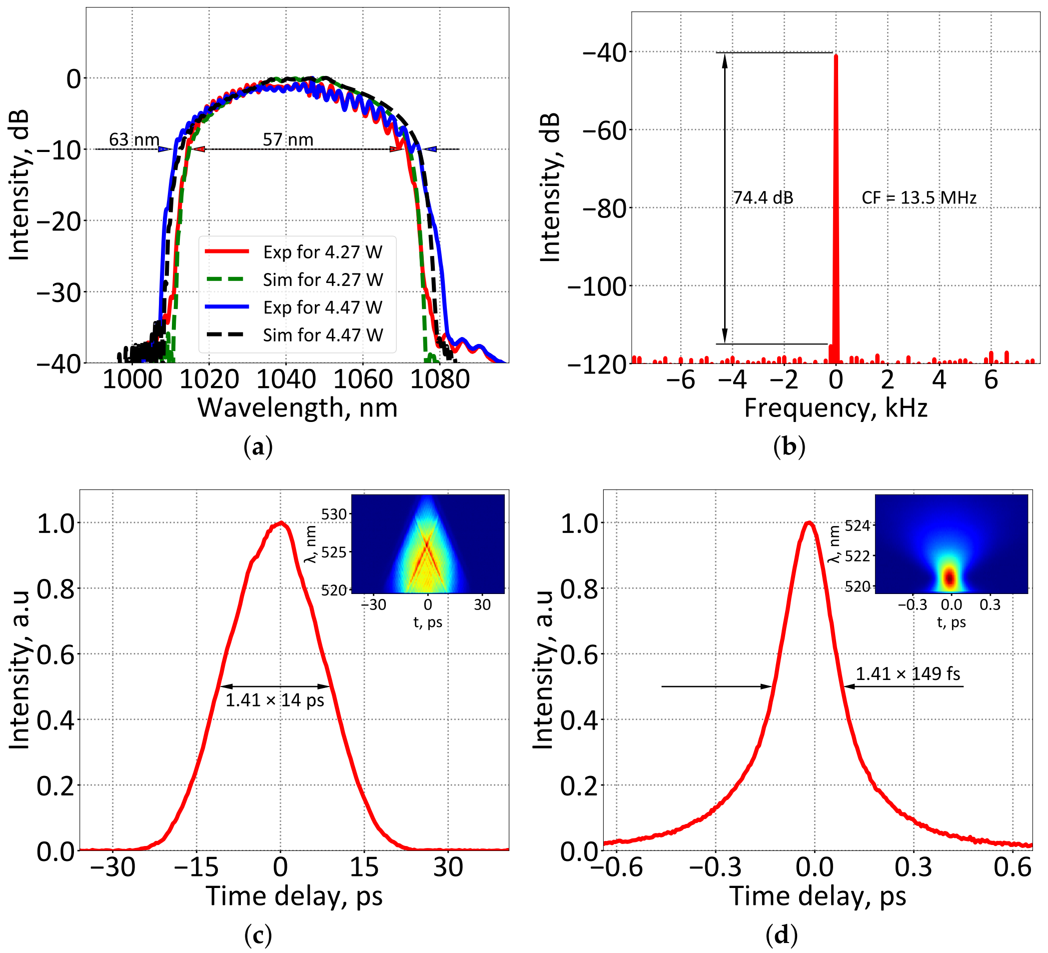

Figure 2. Parameters of the pulses: normalized optical spectra for the 4.3 W of the pump power (solid red line) and 4.5 W (solid blue line), the dashed lines represent the results of numerical simulations (**a**); RF spectrum (**b**), CF—central frequency; autocorrelation function with corresponding FROG trace (inset) for the chirped pulse (**c**) and compressed one (**d**).

3. Numerical Model

The modeling scheme of the experimental setup (Figure 1a) is shown in Figure 3. The propagation of the laser radiation in the fibers was modeled using the generalized nonlinear Schrodinger equation [33], including the Raman scattering term based on the multiple-vibrational-mode model [34] realized by the PyOFSS library [35]. YDF, SMF, and PMF were modeled as single-mode fibers without taking into account the effect of birefringence with the following parameters: $\beta_2 = 22\ \mathrm{ps}^2/\mathrm{km}$, $\beta_3 = 0.037\ \mathrm{ps}^3/\mathrm{km}$, $\gamma = 6\ (\mathrm{W} \times \mathrm{km})^{-1}$. The full-width of the spectral filter at the half-maximum was chosen to be 1.63 nm. It was centered at 1043.3 nm and had a loss of 50% according to the experimentally measured values. An amplification was modeled as a point action gain function with the saturation effect according to:

$$g(E) = \frac{g_0}{1 + E/E_{\mathrm{sat}}}, \tag{1}$$

where g_0 is the gain factor in dB, E is the pulse energy, $E_{\mathrm{sat}} = P_{\mathrm{sat}} \times T_R$ is the saturation energy, and T_R is the cavity round trip time. NPE mode-locking was realised by a simple scalar model [36] which had been proven by a direct comparison with the vector one [37]. It can be represented as a point-action nonlinear self-amplitude modulator (SAM) with a transmission function $\rho(P)$, which is expressed in the following form:

$$\rho(P) = \rho_{\mathrm{max}} - \left(\frac{P}{P_{\mathrm{cr}}} - 1\right)^2 (\rho_{\mathrm{max}} - \rho_{\mathrm{min}}), \tag{2}$$

where $\rho_{\min}$ characterizes the minimal transmission at low powers, and $\rho_{\max} = 0.8$ is the maximum transmission at the critical power P_{cr}. The values for $\rho_{\min}$ and P_{cr} were varied during the simulation.

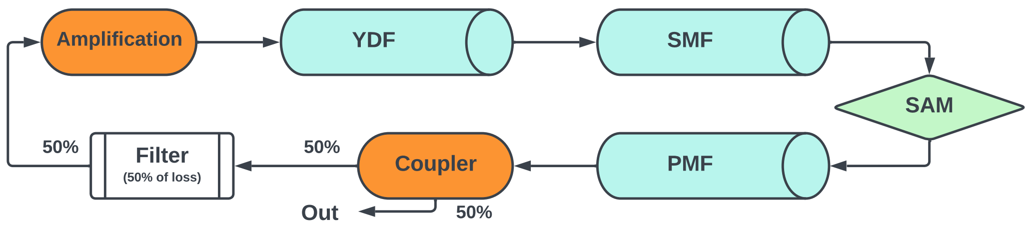

Figure 3. The algorithm used for the simulations of the experimental setup. YDF—double-clad Yb-doped fiber, SMF—single-mode fiber, PMF—polarization-maintaining fiber, SAM—self-amplitude modulator.

The simulation algorithm was as follows. Initially, noise was fed into the cavity just after the coupler. Next, the action of each element was applied one by one to the obtained field. A steady-state soliton was typically formed after 150–200 round trips. It was determined by the relative change in the energy and spectrum width of the pulse.

4. Discussion

We managed to find, numerically, a suitable generation regime with the following parameters: $P_{cr} = 1.9$ kW, $g_0 = 25$ dB, $P_{sat} = 0.3$ mW, and $\rho_{\min} = 0.032$. The obtained spectral shape and pulse duration are in an excellent agreement with the experimental data (see Figure 2a). The evolution of the pulse duration and spectral bandwidth inside the cavity are presented in Figure 4 both at the full-width half-maximum (−3 dB) and −10 dB levels. It can be seen that the spectral broadening happens mostly just after the gain section in a relatively short SMF part of the cavity due to the strong self-phase modulation effect. Since the pulses have a nearly parabolic shape defined by the filter (see Figure 1b), they propagate self-similarly [38]. As a result, the bandwidth increased almost by twenty times (up to 30 nm) without optical wave breaking. After the SAM action, the pulse undergoes mainly dispersion broadening and the duration increases from 2.5 ps to more than 15 ps.

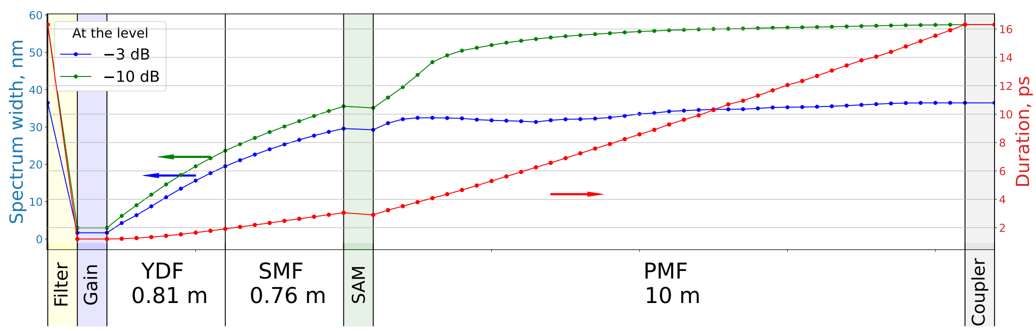

Figure 4. Numerical simulation of the pulse evolution inside the laser cavity.

With varying parameters such as $\rho_{\min}$ and P_{sat}, the area of the stable operation regimes was found in terms of the pulse energy (Figure 5a) and its spectral bandwidth (Figure 5b). It is clearly seen that the spectrum width, which corresponds to the minimal duration of the compressed pulse, is directly related to the pulse energy. So, it is provided by the nonlinear spectral broadening effect in a passive fiber. At the same time, the maximal pulse energy is limited by the value of $\rho_{\min}$ from the right side of the area and by the Raman threshold from the top one. It should be noted that the Raman term in the numerical model plays only a limited role and does not affect the shape of the stable solutions.

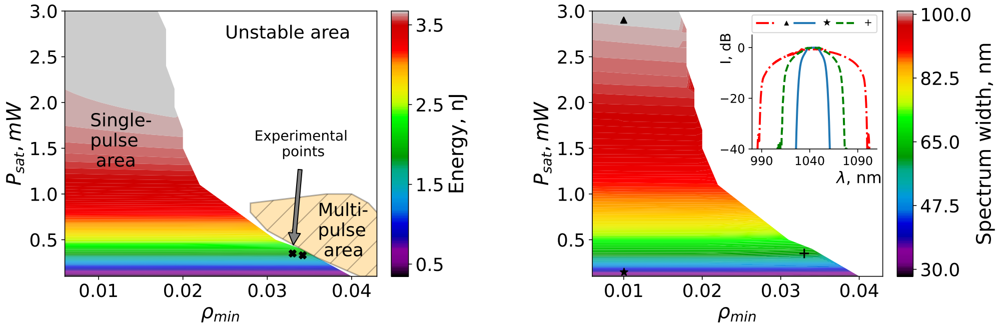

(**a**) (**b**)

Figure 5. Parameters of the pulses of stable area: energy of single-pulse and multi-pulse areas (**a**) and spectrum width at the level of −10 dB (**b**). The crosses indicate the regimes corresponding to the experiment. Inset: spectral shapes in points marked by triangle, star, and cross.

The presented area shows that higher energy can be obtained only by reducing $\rho_{\min}$. This is a quite surprising result in terms of what has been shown previously [37] as the main interaction point corresponding to the pulse peak power is far away from the ground. This is also confirmed here by the absence of any dependence of energy or spectral bandwidth (the same colors are horizontal in Figure 5). So, the $\rho_{\min}$ coefficient does not affect the generated pulse parameters directly. In fact, $\rho_{\min}$ provides the transmission coefficient for a low-power spontaneous emission and pulse tails which are amplified a lot further. Thus, as well as increasing the amplification coefficient in order to obtain more powerful pulses with a broader spectrum, we also amplified the pulse tails further, which reached a steady state over the round trips and formed a multi-pulse operation regime (the shaded area in Figure 5a). To compensate for the effect of an increased gain on low-power radiation, it is necessary to reduce the $\rho_{\min}$ value. Thus, the most unexpected parameter plays the same important role as the length of the SMF part and the pump power. Similar behavior was observed in the Mamyshev oscillator [7,21] where detuned spectral filters provide an almost zero tolerance to low-power radiation. So, we believe that precisely this feature, which is known as zero low-power transmission, has allowed the scaling to be so successful. In our case, it could be possible to obtain a 100 nm pulse generation by reducing the $\rho_{\min}$ down to 1.5% (triangle at the Figure 5b), which corresponds to the transform-limited pulse duration of 36 fs. It should be noted that achieving such a small value of $\rho_{\min}$ in an experiment is a subject for further investigations as the limiting factors are still unknown. Moreover, even the achieved level of less than 4% is rather unusual for an NPE-based SAM and provides a new perspective on the development of a fiber master oscillator. This will certainly result in a new class of high-power ultrashort fiber lasers thanks to the use of modern fiber amplifiers, including those based on tapered fibers [28].

5. Conclusions

A dissipative soliton NPE mode-locked Yb-doped fiber laser has been investigated experimentally and numerically. Shortening the SMF part of the cavity, using a high-power multimode pump, and the fine adjustments made to the PC resulted in a stable operation with a broadband spectrum (over 60 nm) and a relatively high pulse energy (of about 2 nJ). The dechirped pulse duration is about 149 fs, so the chirp parameter is almost 100. The results of the numerical simulations are in a complete agreement with the experimental data. The developed model discovers the reason of such outstanding parameters and predicts, for the first time to our knowledge, the possibility of a 100 nm broad pulse generation by reducing the low-power transmission coefficient of the SAM, which prevents a transition to multi-pulse operation regimes with an increasing pump power. This is a way to produce ultrashort pulses of a sub-100 fs duration as the energy can be multiplied by increasing the mode field diameter of the fibers in the same scheme [12].

Moreover, such a regime could be used to improve the performance of femtosecond fiber laser systems and could also be applied in fields where a broadband laser is required.

Author Contributions: Software, V.D.E.; investigation, S.I.A. and V.D.E.; writing—original draft, S.I.A. and V.D.E.; writing—review and editing, A.G.K., D.S.K. and S.A.B.; supervision, A.G.K. and D.S.K.; funding acquisition, S.A.B. All authors have read and agreed to the published version of the manuscript.

Funding: This work was supported by the state budget of IAE SB RAS (project No 121030500067-5).

Institutional Review Board Statement: Not applicable.

Informed Consent Statement: Not applicable.

Data Availability Statement: Data underlying the results presented in this paper are not publicly available at this time but may be obtained from the authors upon reasonable request.

Conflicts of Interest: The authors declare no conflict of interest.

References

1. Fermann, M.E.; Hartl, I. Ultrafast fibre lasers. *Nat. Photon.* **2013**, *7*, 868–874. [CrossRef]
2. Hoover, E.E.; Squier, J.A. Advances in multiphoton microscopy technology. *Nat. Photon.* **2013**, *7*, 93–101. [CrossRef] [PubMed]
3. Gao, B.; Zhang, R.H.; Huo, J.Y.; Ma, C.Y.; Han, Y.; Hou, Q.R.; Deng, F.; Wu, G.; Ge, Y.Q. Generation and categories of solitons in various mode-locked fiber lasers. *Optik* **2020**, *220*, 165168. [CrossRef]
4. Lefrançois, S.; Kieu, K.; Deng, Y.; Kafka, J.D.; Wise, F.W. Scaling of dissipative soliton fiber lasers to megawatt peak powers by use of large-area photonic crystal fiber. *Opt. Lett.* **2010**, *35*, 1569–1571. [CrossRef]
5. Baumgartl, M.; Jansen, F.; Stutzki, F.; Jauregui, C.; Ortaç, B.; Limpert, J.; Tünnermann, A. High average and peak power femtosecond large-pitch photonic-crystal-fiber laser. *Opt. Lett.* **2011**, *36*, 244. [CrossRef]
6. Jauregui, C.; Limpert, J.; Tünnermann, A. High-power fibre lasers. *Nat. Photon.* **2013**, *7*, 861–867. [CrossRef]
7. Liu, Z.; Ziegler, Z.M.; Wright, L.G.; Wise, F.W. Megawatt peak power from a Mamyshev oscillator. *Optica* **2017**, *4*, 649. Available online: http://xxx.lanl.gov/abs/1703.09166 (accessed on 5 December 2022). [CrossRef]
8. Haig, H.; Sidorenko, P.; Thorne, R.; Wise, F. Megawatt pulses from an all-fiber and self-starting femtosecond oscillator. *Opt. Lett.* **2022**, *47*, 762. [CrossRef]
9. Chong, A.; Buckley, J.R.; Renninger, W.H.; Wise, F.W. All-normal-dispersion femtosecond fiber laser. *Opt. Express* **2006**, *14*, 10095–10100. [CrossRef]
10. Lefrançois, S.; Sosnowski, T.S.; Liu, C.H.; Galvanauskas, A.; Wise, F.W. Energy scaling of mode-locked fiber lasers with chirally-coupled core fiber. *Opt. Express* **2011**, *19*, 3464–3470. [CrossRef]
11. Kharenko, D.S.; Podivilov, E.V.; Apolonski, A.A.; Babin, S.A. 20 nJ 200 fs all-fiber highly chirped dissipative soliton oscillator. *Opt. Lett.* **2012**, *37*, 4104. [CrossRef]
12. Kharenko, D.S.; Gonta, V.A.; Babin, S.A. 50 nJ 250 fs all-fibre Raman-free dissipative soliton oscillator. *Laser Phys. Lett.* **2016**, *13*, 025107. [CrossRef]
13. Wang, Z.; Zhan, L.; Fang, X.; Luo, H. Spectral filtering effect on mode-locking regimes transition: Similariton-dissipative soliton fiber laser. *J. Opt. Soc. Am. B* **2017**, *34*, 2325. [CrossRef]
14. Kharenko, D.S.; Shtyrina, O.V.; Yarutkina, I.A.; Podivilov, E.V.; Fedoruk, M.P.; Babin, S.A. Highly chirped dissipative solitons as a one-parameter family of stable solutions of the cubic-quintic Ginzburg-Landau equation. *J. Opt. Soc. Am. B* **2011**, *28*, 2314–2319. [CrossRef]
15. Ilday, F.O.; Buckley, J.R.; Clark, W.; Wise, F.W. Self-similar evolution of parabolic pulses in a laser. *Phys. Rev. Lett.* **2004**, *92*, 213902. [CrossRef]
16. Dudley, J.M.; Finot, C.; Richardson, D.J.; Millot, G. Self-similarity in ultrafast nonlinear optics. *Nat. Phys.* **2007**, *3*, 597–603. [CrossRef]
17. Zhou, X.; Yoshitomi, D.; Kobayashi, Y.; Torizuka, K. Generation of 28-fs pulses from a mode-locked ytterbium fiber oscillator. *Opt. Express* **2008**, *16*, 7055–7059. [CrossRef]
18. Nie, B.; Pestov, D.; Wise, F.W.; Dantus, M. Generation of 42-fs and 10-nJ pulses from a fiber laser with self-similar evolution in the gain segment. *Opt. Express* **2011**, *19*, 12074–12080. [CrossRef]
19. Iegorov, R.; Teamir, T.; Makey, G.; Ilday, F.Ö. Direct control of mode-locking states of a fiber laser. *Optica* **2016**, *3*, 1312. [CrossRef]
20. Mamyshev, P. All-optical data regeneration based on self-phase modulation effect. In Proceedings of the 24th European Conference on Optical Communication, ECOC '98 (IEEE Cat. No. 98TH8398) Telefonica, Madrid, Spain, 20–24 September 1998; Volume 1, pp. 475–476.
21. Liu, W.; Liao, R.; Zhao, J.; Cui, J.; Song, Y.; Wang, C.; Hu, M. Femtosecond Mamyshev oscillator with 10-MW-level peak power. *Optica* **2019**, *6*, 194. [CrossRef]

22. Ma, C.; Khanolkar, A.; Zang, Y.; Chong, A. Ultrabroadband, few-cycle pulses directly from a Mamyshev fiber oscillator. *Photonics Res.* **2020**, *8*, 65. Available online: http://xxx.lanl.gov/abs/1905.10049 (accessed on 5 December 2022). [CrossRef]
23. Chong, A.; Renninger, W.H.; Wise, F.W. Route to the minimum pulse duration in normal-dispersion fiber lasers. *Opt. Lett.* **2008**, *33*, 2638–2640. [CrossRef] [PubMed]
24. Kharenko, D.S.; Shtyrina, O.V.; Yarutkina, I.A.; Podivilov, E.V.; Fedoruk, M.P.; Babin, S.A. Generation and scaling of highly-chirped dissipative solitons in an Yb-doped fiber laser. *Laser Phys. Lett.* **2012**, *9*, 662–668. [CrossRef]
25. Zhdanov, I.S.; Bednyakova, A.E.; Volosi, V.M.; Kharenko, D.S. Energy scaling of an erbium-doped mode-locked fiber laser oscillator. *OSA Contin.* **2021**, *4*, 2663. [CrossRef]
26. Nyushkov, B.; Kobtsev, S.; Antropov, A.; Kolker, D.; Pivtsov, V. Femtosecond 78-nm Tunable Er:Fibre Laser Based on Drop-Shaped Resonator Topology. *J. Light. Technol.* **2019**, *37*, 1359–1363. [CrossRef]
27. Nyushkov, B.N.; Kobtsev, S.M.; Koliada, N.A.; Antropov, A.A.; Pivtsov, V.S.; Yakovlev, A.V. Mode-locked fibre lasers with an adjustable drop-shaped cavity. *Laser Phys. Lett.* **2017**, *14*, 115101. [CrossRef]
28. Kuznetsov, A.G.; Kharenko, D.S.; Babin, S.A. Amplification of dissipative solitons with a polarisation-maintaining tapered fibre amplifier. *Quantum Electron.* **2018**, *48*, 1105–1108. [CrossRef]
29. Kieu, K.; Renninger, W.H.; Chong, A.; Wise, F.W. Sub-100 fs pulses at watt-level powers from a dissipative-soliton fiber laser. *Opt. Lett.* **2009**, *34*, 593–595. [CrossRef]
30. Lin, J.H.; Wang, D.; Lin, K.H. High energy pulses generation with giant spectrum bandwidth and submegahertz repetition rate from a passively mode-locked Yb-doped fiber laser in all normal dispersion cavity. *Laser Phys. Lett.* **2011**, *8*, 66–70. [CrossRef]
31. Yokokawa, S.; Jin, L.; Set, S.Y.; Yamashita, S. Coherent light source with 106 nm broadband spectrum generated directly from Yb-doped fiber oscillator. In *Fiber Lasers XVII Technology and Systems*; Dong, L., Zervas, M.N., Eds.; SPIE: Bellingham, WA, USA, 2020; Volume 11260, p. 112601L.
32. Trebino, R.; DeLong, K.W. Measuring ultrashort laser pulses in the time-frequency domain using frequency-resolved optical gating. *Rev. Sci.* **1997**, *68*, 3277–3295. [CrossRef]
33. Agrawal, G.P. *Nonlinear Fiber Optics*, 4th ed.; Elsevier: Amsteradm, The Netherlands, 2006.
34. Hollenbeck, D.; Cantrell, C.D. Multiple-vibrational-mode model for fiber-optic Raman gain spectrum and response function. *J. Opt. Soc. Am. B* **2002**, *19*, 2886–2892. [CrossRef]
35. Pyofss: Python-Based Optical Fibre System Simulator. 2021. Available online: https://github.com/galilley/pyofss (accessed on 5 December 2022).
36. Bednyakova, A.E.; Babin, S.A.; Kharenko, D.S.; Podivilov, E.V.; Fedoruk, M.P.; Kalashnikov, V.L.; Apolonski, A. Evolution of dissipative solitons in a fiber laser oscillator in the presence of strong Raman scattering. *Opt. Express* **2013**, *21*, 20556–20564. [CrossRef] [PubMed]
37. Bednyakova, A.E.; Kharenko, D.S.; Yarovikov, A.P. Numerical analysis of the transmission function of the NPE-based saturable absorber in a mode-locked fiber laser. *J. Opt. Soc. Am. B* **2020**, *37*, 2763. [CrossRef]
38. Kruglov, V.I.; Thomsen, B.C.; Dudley, J.M.; Harvey, J.D. Self-similar propagation and amplification of parabolic pulses in optical fibers. *Phys. Rev. Lett.* **2000**, *84*, 6010–6013.